JOURNAL OF NANO- AND ELECTRONIC PHYSICS
Vol. **18** No 2, 02013(6pp) (2026)

ЖУРНАЛ НАНО- ТА ЕЛЕКТРОННОЇ ФІЗИКИ
Том **18** № 2, 02013(6cc) (2026)

OPEN ACCESS

REGULAR ARTICLE

Chipless Orientation Independent RFID Tags Using Square Slot Ring Structures

D. Mondal[1], S. Bhunia[2,*]

[1] *Principal, Kumarganj College, Gour Banga University, West Bengal, India*
[2] *Department of ECE, Central Institute of Technology Kokrajhar, Assam, India*

(Received 20 January 2026; revised manuscript received 21 April 2026; published online 29 April 2026)

RFID is rapidly transforming identification technologies, but reducing tag cost is very essential for replacing conventional barcodes. To address this, researchers are advancing chipless RFID solutions, including reconfigurable square slot ring resonator-based tags. This work presents and compares four configurations of square 4-bit tag designs. The proposed tags are simulated on FR-4 substrate ($\epsilon_r = 4.3, tan\delta = 0{,}025$) with height 0.8 mm and can be mounted on paper, plastic, or implanted in ID cards and bank notes, enabling tracking of up to 16 products. Proposed chipless RFID tag is designed and simulated using CST Microwave Studio 2018. The tag is excited by a plane wave, and the backscattered signal is received by an RCS probe at 100 mm away from the tag to receive the backscattered signal at the far-field region. The proposed tag is symmetric, fully passive, planar, and operate in the multi frequency domain, enabling orientation-independent reading by RFID interrogators. Simulation results demonstrate RF barcode performance across the Ultra-Wideband range (3.1-10.6 GHz), including tag responses under different angular excitations. The proposed concept has been validated by exciting the proposed tag from four different angles – 0°, 30°, 45°, and 60°. In all cases, the results remain nearly identical, demonstrating angular stability. Furthermore, the tags are reconfigurable, and their physical size can be maintained while encoding either a higher or lower number of bits. Owing to these features, the proposed tags are well suited for low-cost tracking applications such as banknotes, postal cards, and ID cards.

Keywords: RFID, Chipless RFID, SRR, Square Slot Ring.

DOI: 10.21272/jnep.18(2).02013 PACS number: 84.40.Ba

1. INTRODUCTION

Radio Frequency Identification (RFID) has emerged as a versatile technology for modern identification, tracking, and security applications, offering significant advantages over conventional optical barcode systems [1]. Barcodes remain inexpensive but they are lacking of non-line-of-sight (NLOS) capability and require human intervention, whereas RFID offers higher data capacity, security, and automated operation. RFID enables wireless and automated data acquisition, supports long interrogation distances without line-of-sight (LOS) alignment between reader and tagged item [2-4]. But it suffers from high tag cost due to the embedded ASIC chip. By removing the ASIC and relying solely on passive electromagnetic structures, using fully passive battery-less tags, chipless tags substantially reduce implementation costs while remaining suitable for applications such as ID cards, tickets, currency notes, and document authentication [5]. However, this cost reduction often comes with reduced encoding capacity and design challenges that must be addressed for practical deployment [6]. Among the available chipless RFID techniques, time-phase-frequency-domain approaches frequency-domain encoding has shown superior data density by representing bits through the presence or absence of resonant frequency signatures [7]. Slot ring resonator-based structures, in particular, offer advantages such as compact size, simple geometry, high coding potential, orientation-independent operation, and compatibility with planar fabrication processes [8-11]. UWB (3.1-10.6 GHz) chipless RFID has emerged as a promising direction due to its low power, multipath immunity, and broad-spectrum availability [12-13]. Motivated by these factors, this paper presents the design and analysis of UWB chipless RFID tags based on square slot ring resonators. Several structural variations are investigated to improve resonant behaviour, and their radar cross-section (RCS) responses are evaluated through simulation. The comparative results enable identification of an optimized resonator configuration suitable for robust and low-cost chipless RFID applications.

2. BASIC OPERATION

A slot etched within a metallic patch resonates at its self-resonant frequency, producing a slot resonator that can be realized in various geometries (horizontal, vertical, circular, square) depending on design constraints and encoding needs [14]. In this work square slot-ring resonators are chosen for their structural advantages. First, the geometric symmetry of these

* Correspondence e-mail: bhuniasunandan@gmail.com

Cite this article as: D. Mondal et al., *J. Nano- Electron. Phys.* 18 No 2, 02013 (2026) https://doi.org/10.21272/jnep.18(2).02013

resonators yields orientation-independent spectral signatures, allowing the tag to be read reliably regardless of angular alignment with the reader [15]. Second, the continuous and symmetric nature of properly designed slot ring resonators suppresses spurious resonances so that the backscattered response is dominated by the intended fundamental mode; this simplifies spectral interpretation and reduces mis-reads caused by harmonic clutter [16]. Third, slot ring geometries enable relatively high bit-encoding capacity per unit area because multiple resonances (or tunable resonator elements) can be accommodated within a compact patch footprint, improving coding density for UWB frequency-domain tags [17]. The following subsections present the mathematical formulations and design equations for square slot ring resonators used in this study.

Square Slot Ring Resonators

As seen from the theory of circular slot ring resonator, wavelength (λ_g)can be expressed as

$$\lambda_g = 2(L_i + L_i - 2W_i) \quad (1)$$

$$L_i = L_{i-1} - W_{i-1} - G_{i-1} \quad (2)$$

Where L_i is side length for i^{th} resonator, W_i is width of corresponding slot and G_i is gap between two slots.

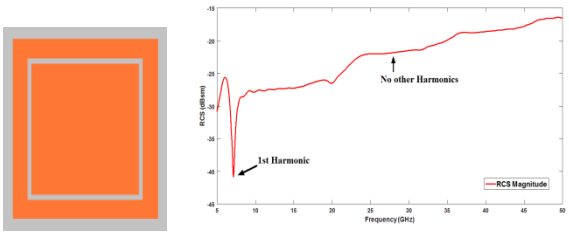

a b

Fig. 1 – Backscatter frequency response plot of a square slot ring resonator inside a patch

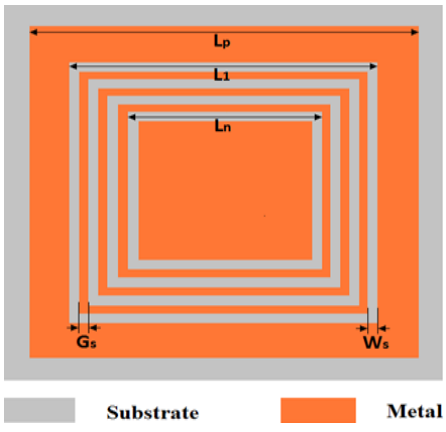

Fig. 2 – Square orientation-less chipless RFID tag

The resonance frequency (f_i) of a squares slot ring resonator with side length L_i and slot width W_i can be approximated in Eq. 3 [18].

$$f_i = \frac{c}{2(L_i+L_i-2W_i)}\sqrt{\frac{2}{\varepsilon_r+1}} \quad (3)$$

Where c is the velocity of light, ε_r is relative permittivity of substrate. The outline of an N-bit tag is shown in the Figs. 1-2 with dimension as parameters for resonance frequency calculation. Here W_s is width of a slot, G_s is gap between two adjacent slots and L_n is length of nth slot and L_p is the length of outer patch. Use of N concentric square slot ring resonators will produce N different resonance frequencies.

Tag Measurement

Practically, measurement of the backscattered power from the tag in the far-field is carried out using Vector Network Analyzer (VNA). There are two possible measurement configurations: the bi-static bench with two antennas and the mono-static bench with only one antenna. The backscattered power transfer is characterized by the transmission coefficient in bi-static bench and the reflection coefficient in mono-static bench.

2.1 Bi-Static Measurement

The emitted wave has an incident angle α in the bi-static configuration. The radiation pattern of the tag is quasi-omnidirectional so in RFID tags this angle does not affect the measured Radar Cross Section (RCS). The basic configuration of bi-static measurement is given in Fig. 3. Actually, the RCS can be determined by measuring the power of backscattered and using the radar equation. In this equation transmitting power and receiving power have relation given in Eq. 4 [15].

$$P_r = \frac{P_t G_t G_r \lambda^2 \sigma_{tag}}{(4\pi)^3 R^4} \quad (4)$$

Where P_t is transmitting power, P_r is receiving power, G_t, G_r are respectively gain of Transmitter and Receiver, λ is transmitting wavelength, R is distance between antenna and tag, σ_{tag} is the RCS of the tag. The power transferred from Port 1 to Port 2 is given by Eq. 5.

$$\frac{P_r}{P_t} = |S_{21}|^2 \quad (5)$$

So, the RCS of the tag can be expressed as in Eq. 6 [15].

$$\sigma_{tag} = |S_{21}|^2 \frac{(4\pi)^3 R^4}{G_t G_r \lambda^2} \quad (6)$$

It can be observed from Eq. 6, S_{21} parameter of a tag has a direct relationship with RCS of that tag. This fact is very much important for tag simulation perspective as the whole simulation is done using RCS measurement in Computer Simulation Technology (CST) Microwave Studio.

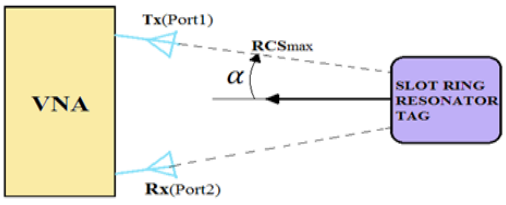

Fig. 3 – Configuration of Bi-static Measurement Set-up Bench

2.2 Mono-Static Measurement

The mono-static setup is basically for the tags which are excited by normally incident plane wave. However, the setup introduces the superposition of the reflected wave from the Transmitter/Receiver antenna to the backscattered wave from the tag. The basic calculations for mono-static measurement are almost similar to that of bi-static measurement. So, the relation between received and transmitted power is can be expressed by Eq. 7.

$$P_r = \frac{P_t G_t{}^2 \lambda^2 \sigma_{tag}}{(4\pi)^3 R^4} \quad (7)$$

Where P_t is transmitting power, P_r is receiving power, G_t is gain of Transmitter and Receiver, λ is transmitting wavelength, R is distance between antenna and tag, σ_{tag} is the RCS of the tag. The return loss (S_{11}) can be portrayed by Eq. 8.

$$\frac{P_r}{P_t} = |S_{11}|^2 \quad (8)$$

Using Eqs. 7, 8 RCS of tag can be calculated by Eq. 9 [4].

$$\sigma_{tag} = |S_{11}|^2 \frac{(4\pi)^3 R^4}{G_t{}^2 \lambda^2} \quad (9)$$

The similarity of bi-static and mono-static measurement is evident from these above-mentioned equations. In this paper, both the two types of simulation are done. One is done by exciting the chipless RFID tags by normally incident plane wave. For that case, mono-static RCS measurement process calculations are considered. On the contrary, when simulations are done using plane wave with a finite incident angle α, bi-static measurement technique calculations are used.

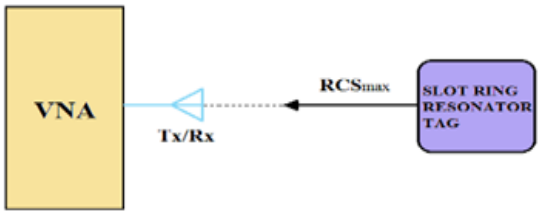

Fig. 4 – Configuration of mono-static measurement set-up bench

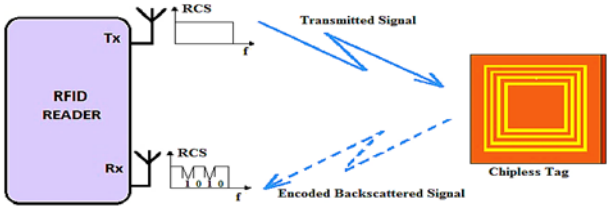

Fig. 5 – Operating principle of squared shaped tags

Operating Principle

The operating principle is illustrated in Fig. 5. The tag is excited by the signal transmitted from a linearly-polarized transmitting antenna (T_x). As a result, a frequency selective behavior with sharp dips is observed in the vicinity of the resonant frequencies in the backscattered signal. This signal is received by another linearly-polarized receiver antenna (R_x) at the reader. As the tag is symmetric to the reader antenna, the frequency encoded behavior is independent of orientation of the tag.

3. DESIGN OF CHIPLESS RFID TAG

A chipless RFID tag is designed and simulated using CST Microwave Studio 2018. The tag is excited by a plane wave, and the backscattered signal is received by an RCS probe at 100 mm away from the tag to receive the backscattered signal at the far-field region. Fig. 6 describes the simulation set up where the tag is excited from an angle. The angle of excitation is denoted by α. Frequency selective behavior is obtained when a plane wave excites the tag. This behavior is denoted by sharp dips at the corresponding resonant frequencies. In this paper, four-bit RFID tags are designed which can be used to track at most sixteen products. But the number of bits can be increased by incorporating a greater number of slot rings within the patch. Logic state of a bit can be changed by simply shorting the corresponding slots which will eliminate those particular frequencies from the backscattered signal. So, the exclusion of frequency is denoted as logic '0' whereas the presence of the frequency is considered as logic '1'. Ring number 1 has the longest length with the lowest frequency, which is denoted as MSB whereas ring number 'n' with the highest frequency is denoted as LSB.

The tag is simulated on FR-4 substrate ($\epsilon_r = 4.3, tan\delta = 0{,}025$) with height 0.8 mm and can be mounted on paper, plastic, or implanted in ID cards and bank notes, enabling tracking of up to 16 products. The design parameters for the slot ring resonators are: $G_s = W_s = 0.15$ mm, MSB frequency = 6 GHz, $R_p = 6.80$ mm, and $L_p = 15.40$ mm. Simulation frequency bands is 5.5 – 11.5 GHz. Other parameters are calculated using Eqs. 1-3 in Table 1.

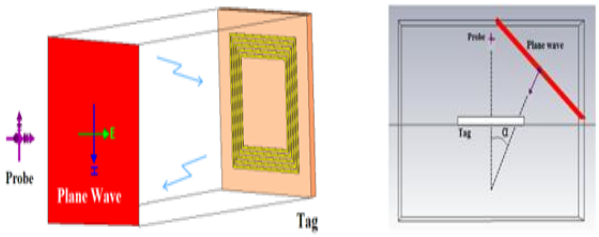

a b

Fig. 6 – Simulation setup for SRR chip-less RFID tags

Table 1 – Slot ring parameters

Shape	Parameters	Dimensions(mm)
Square slot ring resonator	L_1	7.83
	L_2	7.23
	L_3	6.63
	L_4	6.03

For the normal structure of slot ring resonator-based chipless RFID for geometrical shape shown in Fig. 2 the values are tabulated in Table 2, B_3 and B_0 denote MSB and LSB respectively. It has been observed from the Table 2 that the simulated frequency of LSB for square shape deviates 17.47 % from the calculated frequency. This deviation is much higher than that of

the other bits. Fig. 7 depicts the graphical representation of the same.

Table 2 – Bit representation of normal structure

Shape	Bits	Calculated Freq (GHz)	Simulated Freq (GHz)	Absolute Error (%)
Square	B_3	6.00	6.20	3.33
	B_2	6.51	6.77	3.99
	B_1	7.11	7.46	4.92
	B_0	7.84	9.21	17.47

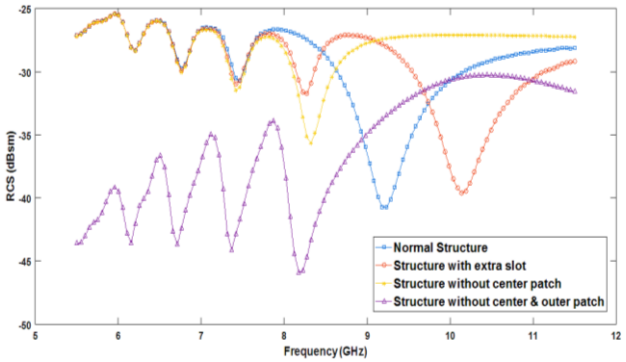

Fig. 7 – Simulation results for different configurations of square slot ring resonator

The high percentage error regarding frequency of LSB of the structure is the main drawback. Hence, the concept of removing the center patch comes into picture. This configuration for square shape is illustrated in Fig. 8 (a). It helps in improvement of LSB frequency. It can be seen from Table 3, the percentage errors of LSB comes down to 5.99 %. For a better perception, Fig. 7 can be referred. Clearly, these observations indicate that the LSB frequencies have improved as compared to the previous one. By adding an extra dummy slot inside the innermost slot depicted in Fig. 8(b) this result in the improvement in percentage error from 5.99 % to 5.22 % (Table 4). But this particular configuration has not produced overall desired result. Finally, the structure without center and outer patch, shown in Fig. 8(c) is simulated. It is observed from Fig. 7 that the results obtained are the best among all the mentioned configurations. The improvement in error of LSB is 4.33 % (Table 5) for square shapes.

Table 3 – Bit Representation of Structure without Center Patch

Shape	Bits	Calculated Freq (GHz)	Simulated Freq (GHz)	Absolute Error (%)
Square	B_3	6.00	6.20	3.33
	B_2	6.51	6.77	3.99
	B_1	7.11	7.44	4.64
	B_0	7.84	8.25	5.99

Table 4 – Bit representation of structure with extra slot

Shape	Bits	Calculated Freq (GHz)	Simulated Freq (GHz)	Absolute Error (%)
Square	B_3	6.00	6.20	3.33
	B_2	6.51	6.77	3.99
	B_1	7.11	7.44	4.64
	B_0	7.84	8.25	5.22

Table 5 – Bit representation of structure without center & outer patch

Shape	Bits	Calculated Freq (GHz)	Simulated Freq (GHz)	Absolute Error (%)
Square	B_3	6.00	6.12	2.00
	B_2	6.51	6.70	2.91
	B_1	7.11	7.36	3.51
	B_0	7.84	8.18	4.33

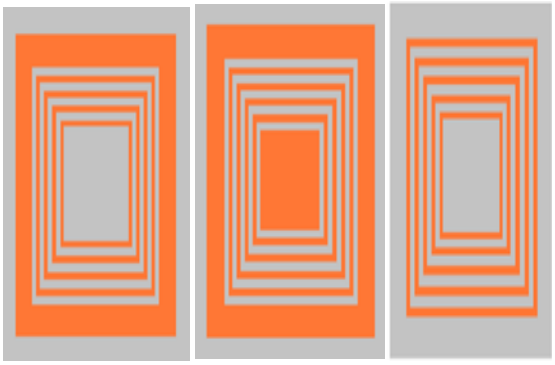

Fig. 8 – Different configurations of square chipless tag

3.1 Finalizing the Ultimate Configuration

It is evident from the above comparison that the structures without the center and outer patch for both the shapes are producing the best result among all other configurations. Based on these results, structure without the center and outer patch is chosen to design four different tag IDs of each shape. These four tags are presented in Fig. 9. As seen from Fig. 9 (a) the presence of all the four slots denotes tag ID '1111'. On the contrary, in the Fig. 9 (b) all the four slots are shorted together to get the ID '0000'. Fig. 9 (c) shows ID '0101', which is created by shorting 1st and 3rd slots. Similarly, shorting 2nd and 4th slots result in ID '1010', which is illustrated in Fig. 9 (d).

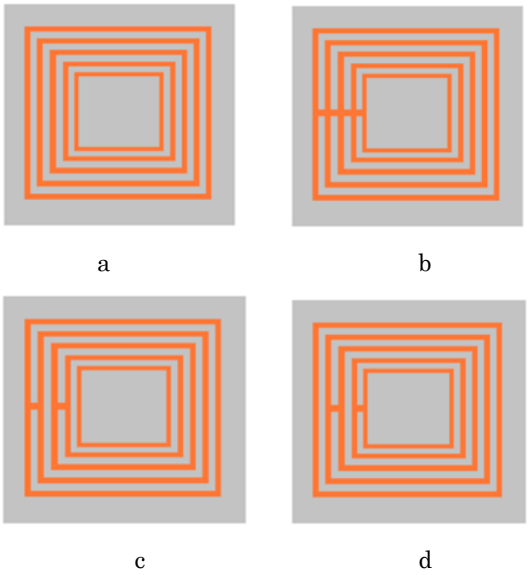

Fig. 9 – Simulated Tags with Different IDs, (a) – Tag ID '1111', (b) – Tag ID '0000', (c) – Tag ID '0101', (d) – Tag ID '1010'

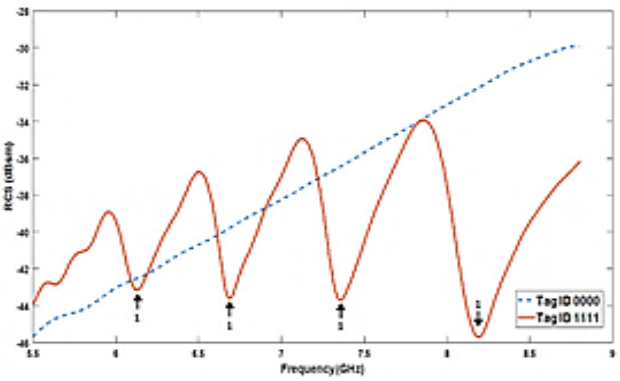

Fig. 10 – Simulation results for tags in Fig. 9 (a, b)

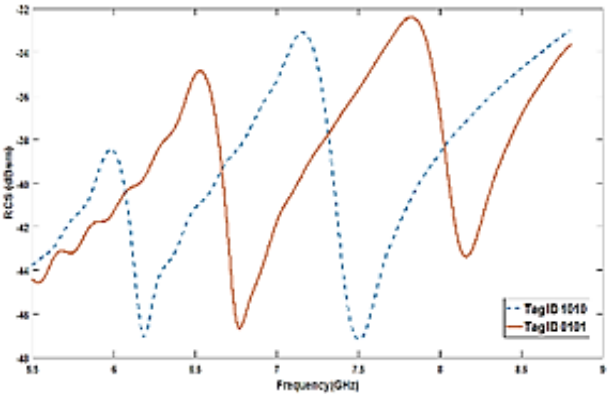

Fig. 11 – Simulation results for tags in Fig. 9 (c, d)

3.2 Angular Excitation of Tags

Previously, the simulation results of tags under perpendicular excitation have been discussed in Fig. 7. Here, the graphical comparisons of tags with angular excitation are discussed. Angular excitation can be given over angle from 0° to 90° and 0° to – 90°. Due to symmetry of tag, only one range, i.e. 0° to 90°, has been considered for simulation. Lastly the tags shown in Fig. 9 (a-d) are simulated at 30°, 45° and 60° angular excitation. The respective results are illustrated in Fig. (12-15). The outcome is identical and the maximum RCS is achieved for perpendicular i.e. 0° excitation in this case also. Hence, from the above observation, it can be stated that slot ring resonators are orientation independent.

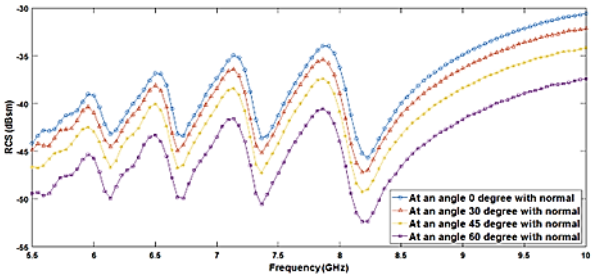

Fig. 12 – Simulation results for Fig. 9 (a)

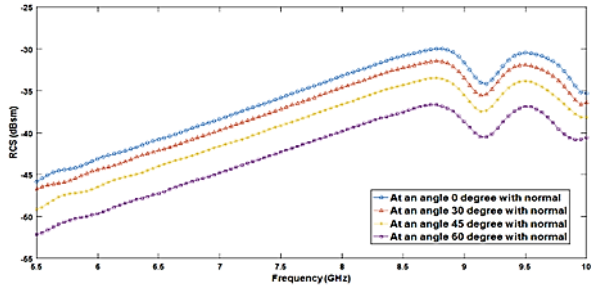

Fig. 13 – Simulation results for tags in Fig. 9 (b)

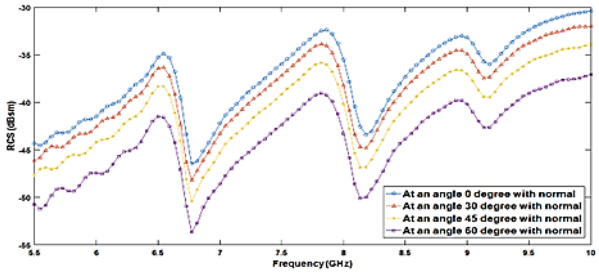

Fig. 14 – Simulation results for tags Fig. 9 (c)

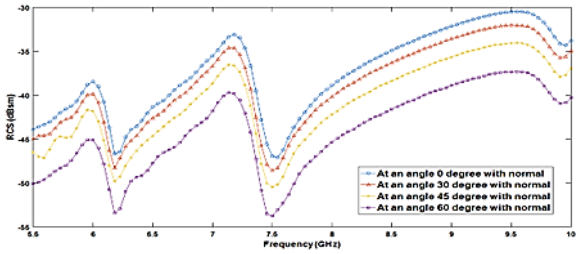

Fig. 15 – Simulation results for Fig. 9 (d)

4. CONCLUSION

RFID system using Slot Ring Resonator is illustrated in this paper. The slot ring resonators can be of different shapes but here square slot resonator is taken into consideration. The frequency signature can be obtained from backscattered signal of the tag. Backscattered power measurement method is also discussed here. To get the desired frequency band, some modification in the square slot ring resonator has been introduced. The comparison between each structure has been shown and the best among those four configurations is chosen for encoding and application. Slot ring resonators are symmetric in nature hence they provide similar result with any alignment. This concept has been elaborated and justified by exciting the tag from four different angles – 0°, 30°, 45° and 60°. For each case, the result is more or less identical. Also, these tags are reconfigurable and size of the tag can be kept same to encode higher or lesser number of bits. Therefore, these are suitable for low-cost tracking applications like banknotes, postal cards, ID cards etc.

REFERENCES

1. K. Finkenzeller, *RFID Handbook: Fundamentals and Applications in Contactless Smart Cards, Radio Frequency Identification and Near-Field Communication, 3rd Ed.* (New York, NY, USA: Wiley: 2010).
2. D.M. Dobkin, S.M. Weigand, *IEEE MTT-S Int. Microwave Symp. Digest* **2**, 135 (2005) https://doi.org/10.1109/MWSYM.2005.1516541.
3. S. Preradovic, N.C. Karmakar, *IEEE Microwave Magazine* **11** No 7, 87 (2010) https://doi.org/10.1109/MMM.2010.938571.
4. S.S. Sarma, *Proc. IEEE SoutheastCon* (2008).
5. N.C. Karmakar, E.M. Amin, J.S. Bhuiyan, *Chip less RFID Sensors* (Hoboken, NJ, USA: Wiley: 2016).
6. E.M. Amin, J.S. Bhuiyan, M.S. Uddin, N.C. Karmakar, *IEEE Access* **4**, 1 (2016).
7. S. Preradovic, I. Balbin, N.C. Karmakar, G.F. Swiegers, *IEEE Trans. Microwave Theory Tech.* **57** No 5, 1411 (2009) https://doi.org/10.1109/TMTT.2009.2017323.
8. I. Jalaly, D. Robertson, *IEEE International Symposium on Microwave, Antenna, Propagation and EMC Technologies for Wireless Communications,* 232 (2005).
9. S.M. Islam, M.S. Uddin, N.C. Karmakar, *IEEE Sensors J.* **15** No 10, 5573 (2015).
10. M. Noman, U. Haider, H. Ullah, A. Hashmi, F. Tahir, *IEEE J. Radio Frequency Identification* **6**, 671 (2022) https://doi.org/10.1109/JRFID.2022.3211301.
11. E. Dogan, A.K. Gorur, A. Gorur, *IEEE Access* **11**, 107429 (2023) https://doi.org/10.1109/ACCESS.2023.3320108.
12. M. Noman, U.A. Haider, H. Ullah, M. Ikram, H. Rmili, F.A. Tahir, *Electronics* **12** No 6, 1371 (2023) https://doi.org/10.3390/electronics12061371.
13. M.G. Di Benedetto, T. Kaiser, A. Molisch, I. Oppermann, C. Politano, D. Porcino, *UWB Communications Systems: A Comprehensive Overview* (New York, NY, USA: Hindawi: 2006).
14. N. Huang, S. Preradovic, N.C. Karmakar, *Electronics* **10**, 9 (2021).
15. M.A. Islam, Y. Yap, N. Karmakar, A. Azad, *Progr. Electromagn. Res. C* **33**, 55 (2012) http://dx.doi.org/10.2528/PIERC12071306.
16. C.-C. Le, T.-K. Dao, N.-Y. Pham, T.-H. Nguyen, *Sensors* **24**, 4435 (2024) https://doi.org/10.3390/s24144435.
17. M. Noman, *Electronics* **12** No 6, 1371 (2023) https://doi.org/10.3390/electronics12061371.
18. D.K. Barton, *IEEE Trans. Aerosp. Electron. Syst.* **36** No 2, 356 (2000) https://doi.org/10.1109/TAES.1972.309475.

Незалежні RFID-мітки без орієнтації чіпа з використанням кільцевих структур з квадратними щілинами

D. Mondal[1], S. Bhunia[2]

[1] *Principal, Kumarganj College, Gour Banga University, West Bengal, India*
[2] *Department of ECE, Central Institute of Technology Kokrajhar, Assam, India*

RFID швидко трансформує технології ідентифікації, але зниження вартості міток є дуже важливим для заміни традиційних штрих-кодів. Щоб вирішити цю проблему, дослідники розробляють безчіпові RFID-рішення, включаючи реконфігуровані мітки на основі квадратних щілинних кільцевих резонаторів. У цій роботі представлено та порівняно чотири конфігурації квадратних 4-бітних конструкцій міток. Запропоновані мітки змодельовані на підкладці FR-4 (ϵ_r = 4.3, tanδ = 0,025) висотою 0,8 мм і можуть бути встановлені на папері, пластику або імплантовані в посвідчення особи та банкноти, що дозволяє відстежувати до 16 продуктів. Запропонована безчіпова RFID-мітка розроблена та змодельована за допомогою CST Microwave Studio 2018. Мітка збуджується плоскою хвилею, а сигнал зворотного розсіяння приймається зондом RCS на відстані 100 мм від мітки для прийому сигналу зворотного розсіяння в дальній зоні. Запропонована мітка є симетричною, повністю пасивною, планарною та працює в багаточастотній області, що дозволяє RFID-інтеррогаторам зчитувати дані незалежно від орієнтації. Результати моделювання демонструють продуктивність радіочастотних штрих-кодів у всьому надширокосмуговому діапазоні (3,1-10,6 ГГц), включаючи реакції мітки під різними кутовими збудженнями. Запропонована концепція була підтверджена шляхом збудження запропонованої мітки під чотирма різними кутами – 0°, 30°, 45° та 60°. У всіх випадках результати залишаються майже ідентичними, що демонструє кутову стабільність. Крім того, мітки можна реконфігурувати, а їхній фізичний розмір можна підтримувати при кодуванні як більшої, так і меншої кількості бітів. Завдяки цим особливостям запропоновані мітки добре підходять для недорогих застосувань відстеження, таких як банкноти, поштові картки та посвідчення особи.

Ключові слова: RFID, Безчіпова RFID, SRR, Кільце з квадратним пазом.